Fermi National Accelerator Laboratory

FERMILAB-Conf-89/257-E
[E-741/CDF]

Intermediate Vector Bosons in the Muon Channel *

The CDF Collaboration

presented by

David A. Smith
Instituto Nazionale di Fisica Nucleare - Sezione di Pisa
56010 S. Piero a Grado, Pisa, Italy

December 1989

* Talk presented at the 8th Topical Workshop on $p\bar{p}$ Collider Physics, Castiglione della Pescaia, Italy, September 1-5, 1989.

Operated by Universities Research Association Inc. under contract with the United States Department of Energy

CDF/Pub/EWK/Public 1082

Intermediate Vector Bosons in the Muon Channel

The CDF Collaboration*

Presented by David A. Smith
Istituto Nazionale di Fisica Nucleare – Sezione di Pisa
56010 S. Piero a Grado, Italy

Talk presented at the 8th workshop on Proton-Antiproton Collider Physics, Castiglione della Pescaia (Italy), 1-6 September 1989.

Abstract

Description of the $W^{\pm}$ and Z^0 mass measurement in the muon decay channel, using 4.4 pb^{-1} of proton-antiproton collision data from the Fermilab Tevatron and CDF. A preliminary result of $M_W = 79.9 \pm 0.4 \pm 0.6$ GeV/c^2 is presented, and the published values of $M_Z = 90.9 \pm 0.3 \pm 0.2$ GeV/c^2 and $\Gamma_Z = 3.8 \pm 1.1 \pm 1.0$ GeV/c^2 are described.

* The CDF collaboration is listed in the appendix.

In the Standard Model, the masses and widths of the intermediate vector bosons $W^{\pm}$ and Z^0 are closely related to the weak mixing angle $\sin^2\theta_W$, the mass of the Top quark, and the number of neutrino generations [1]. While the current generation of e^+e^- colliders makes more precise Z^0 measurements [2], the Fermilab Tevatron, producing $p\bar{p}$ collisions at $\sqrt{s} = 1.8$ TeV, provides a unique opportunity to study $W^{\pm}$ production. The Collider Detector at Fermilab (CDF) recorded an integrated luminosity of 4.4 pb^{-1} during the data run ending in June, 1989, and analyses of muon and electron data are well underway. The two lepton channels are complimentary to each other, having different sources of background and systematic errors, and provide independent checks. This paper describes the mass measurements in the muon channel.

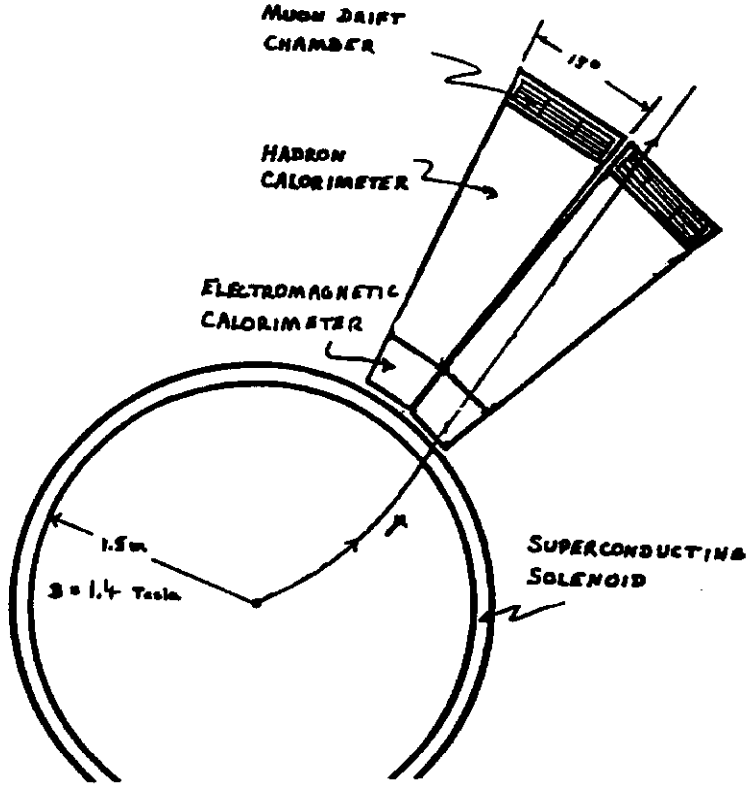

Figure 1: Transverse view of CDF showing the central muon chambers, the calorimeter wedges and the central tracking chamber.

The CDF detector has been described in detail elsewhere [3]. Briefly, CDF is an azimuthally symmetric detector with good solid angle coverage, consisting of high-granularity electromagnetic (EM) hadron (HAD) calorimeters, high-resolution tracking chamber (CTC) in an 1.412 Tesla axial magnetic field, a vertex time projection chamber, and muon tracking. Figure 1 shows the geometry of the muon chambers in the central region (CMU). Sets of muon chambers lie behind 5 interaction lengths of calorimetry,

Cut	Description
Muon Quality	$p_t > 20$ GeV for muon $r\phi$ track match < 1.5 cm $E_{EM} + E_{Had} < 3.5$ GeV in tower hit by muon CTC impact parameter <2.5 mm
QCD jets cut	No jet ($E_t > 5$ GeV) within 30° of back-to-back
No jets	No jet ($E_t > 7$ GeV) anywhere in event
Veto Z°'s and cosmics	No other track with $p_t > 15$ GeV in event

Table 1: Cuts used in selection of $W \rightarrow \mu\nu$ events.

over the angle $56° < \theta < 124°$ from the beam. They have four layers of $\delta\phi \approx 1°$ cells, using charge division to measure the longitudinal track coordinate, z, and drift time for the transverse coordinate $r\phi$. A level-1 trigger rejects low transverse momentum tracks by testing the drift-time difference between alternate layers of the chambers, which amounts to a cut on the bending of the track in the magnetic field. The level-2 trigger matches level-1 muons with high momentum tracks from the central tracking chamber, reconstructed by a fast online processor.

$W \rightarrow \mu\nu$ Analysis

The momentum vector of the neutrino is determined from the energy and momentum imbalance in the detector. Since energy flow down the beampipe is undetectable, the longitudinal component of the neutrino vector is unknown and we cannot study the invariant mass of the muon-neutrino pair, but only the transverse mass,

$$M_t = \sqrt{2p_t^{\mu} p_t^{\nu}(1 - \cos\Delta\phi_{\mu\nu})}$$

where p_t^{μ} and p_t^{ν} are the muon and neutrino transverse momenta, and $\Delta\phi_{\mu\nu}$ is the azimuth angle between the muon and the neutrino. The observed M_t distribution depends on the W transverse momentum distribution, on the detector smearing (resolution) of the lepton momenta, and on the geometrical acceptance of the detector. The p_t of the W's is sensitive to the proton structure functions, since a change in the longitudinal momentum of the W changes the transverse momentum as well. The kinematics of the W decay combined with the structure functions, resolution, and geometry do not lend themselves well to an analytical expression, and therefore we use monte carlo methods to predict the momentum distribution.

The cuts used in data selection must remove any background not modeled by the

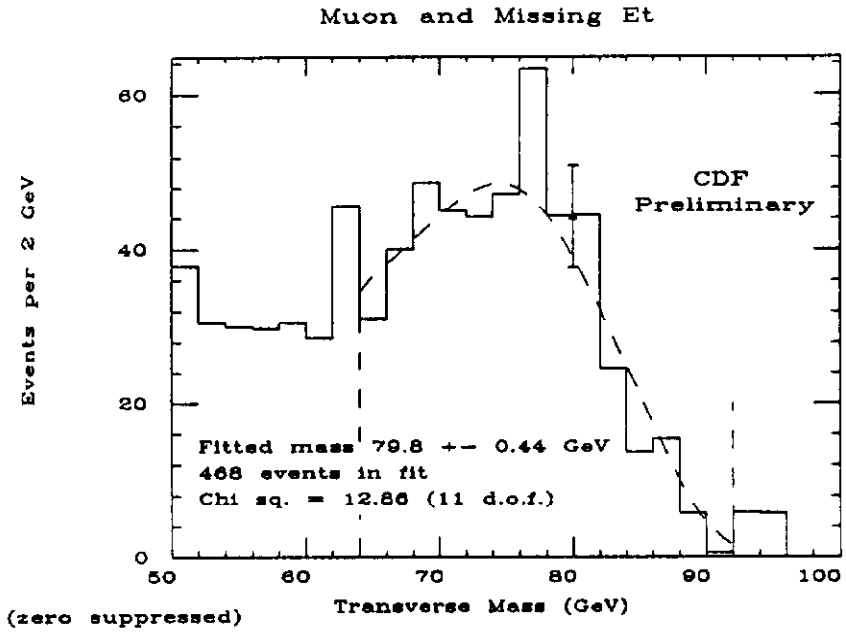

Figure 2: Transverse mass distribution for $W \rightarrow \mu\nu$ candidates. The vertical dashes show the mass range used in the fit, the dashed curve is the result of the fit.

monte carlo without introducing a kinematic bias that would distort the distribution relative to that predicted by calculation. To this end, we apply the cuts listed in table 1 to an inclusive muon sample. The CTC impact parameter is the distance of closest approach of the reconstructed track to the beam in the $r\phi$-plane, and is used in this analysis as a measure of the quality of the track. The muon quality cuts and the QCD jet cut select isolated, well-measured, minimum ionizing particles while rejecting hadron punchthrough from back-to-back jets and muons from B-meson decay. Events with any jet having uncorrected $E_t > 7$ GeV are rejected for consistency with the monte carlo. Our monte carlo generates W and Z bosons from the exact leading order $q\bar{q} \rightarrow W$ diagram using a variety of structure functions and simple parametrizations of the boson P_t [4]. The monte carlo has the advantages of speed, simplicity, and accuracy for the diagram used, but does not include W's with jets. The last cut, vetoing any other high momentum track in the event, removes most Z^0 decays and cosmic rays. Table 2 shows the number of events removed by the various cuts. The choice of cuts has the additional advantage of being similar to the cuts used in the electron analysis, facilitating comparison of the two analyses. After all cuts 892 events remain. Of these,

Z^0, cosmic veto	Jet cuts	Muon Quality	Events	Fraction
			10385	100 (%)
1			5007	48.2
	1		1635	15.7
1	1		1174	11.3
		1	2746	26.4
1		1	2252	21.7
	1	1	1134	10.9
1	1	1	892	8.6

Table 2: Fraction of events passing data selection cuts. A "1" means the cut was applied, an empty box means the cut was not made.

727 have $M_t \geq 50$ GeV, shown in figure 2. For the mass fit of figure 2, only the 468 W candidates in the range $64 \leq M_t \leq 92$ GeV were used.

While rejecting events with a second high momentum track removes Z's where both muon tracks have been reconstructed, events where one of the muons is too far forward for the central tracking chamber are a background to the W signal. The rate is low: the Z^0 cross section is about a tenth of the $W^{\pm}$ cross section [5], and the geometric acceptance is only 20%, so that the Z background is on the order of 0.02 of the W signal. Nonetheless, this background could be critical in that the events favor the high edge of the M_t distribution. To remove this background, we used a monte carlo to study the shape of the M_t distribution when one of the muons from Z decay is undetectable. The distribution was normalized using the number of observed central-central Z's, and then subtracted from the signal. No change in the fitted W mass occurred. Table 3 shows the effect of varying the normalization.

Figure 2 shows a tail above $M_t = 90$ GeV/c^2. There are 19 overflow events. Scanning shows these events to be cosmic rays, events with a second $p\bar{p}$ vertex or an overlapping beam-gas collision, or an unidentified pion or kaon decay-in-flight. The high mass tail indicates that there are still background events in the signal region. At the time of this conference, we were still developing the methods to cleanly reject these tail events. However, to explore their effect, we subtracted backgrounds according to various models and then re-fit the data. We found that the fitted mass did not change within the quoted errors. On the other hand, the fitted width of the distribution is sensitive to the backgrounds. This is the main reason why we are not presenting even a preliminary

Scale Factor	M_W	Normalization	χ^2/dof
0.	79.8	547 ± 23	15.1/13
0.02	79.8	534 ± 23	16.0/13
0.04	79.8	520 ± 23	19.1/13

Table 3: Effect of varying the amount of $Z^\circ \rightarrow \mu^+\mu^-$ background subtraction. The monte carlo transverse mass distribution for single muons from Z° decay is multiplied by the scale factor before subtraction from the $W \rightarrow \mu\nu$ data.

width measurement at this time.

The M_t distribution shows background below $M_t = 60$ GeV. Likely sources are back-to-back jets in the tails of the fragmentation functions along with hadron punchthrough or decay-in-flight, or Beauty decays producing soft, diffuse jets. For the purposes of this paper, the important point is that the fitted mass is insensitive to the W selection cuts or to the background subtraction, within the quoted errors. Table 4 shows that varying the width of the M_t window, which in effect changes the amount of background at the low end, changes the mass by only 400 MeV/c^2.

Fitting Method

Figure 3 shows a set of monte carlo M_t distributions where the W mass was varied from 77.8 to 83.8 GeV/c^2 and the width was fixed at $\Gamma_W = 3.0$ GeV/c^2. A similar set is generated for a range of widths centered at $\Gamma_W = 2.15$ GeV/c^2. The Standard Model prediction for $M_W = 80.0$ GeV/c^2, $\alpha_s = 0.1$, and $M_{top} > M_W - M_b$ is $\Gamma_W = 2.06$ GeV/c^2. CDF has recently measured $\Gamma_W = 2.18 \pm 0.21$ GeV/c^2 [5]. From this grid of mass and width values a χ^2 is calculated as in formula (8) of reference [1], using MINUIT [6].

Figure 4 shows the resulting χ^2 as a function of mass. The most likely mass is at the minimum of the curve, and the width of the dip at one unit of χ^2 above the minimum gives the standard deviation of the mass value. Because of the finite statistics of both the data and the monte carlo distributions, the χ^2 curve is not smooth. Hence the apparent minimum and width can be misleading. For this reason, we fitted a parabola to the χ^2 values, as shown in the figure. Varying the structure functions used to calculate the M_t distribution changes the mass value by 300 MeV/c^2. Finally, a 100 MeV/c^2 correction is added to M_W for photons lost by brehmstrahlung of the muon track and lost due

Fit Interval (GeV)	Fit to Data M_W	Events	χ^2/dof	Fit to Monte Carlo
Width Floated				$(M_W = 80\,, \Gamma_W = 2.8)$
56 - 94	79.8 GeV	609	22.0/16	80.2 ± 0.4 ; 2.2 ± 0.9
60 - 94	79.8	548	21.9/14	80.1 ± 0.3 ; 2.8 ± 0.4
64 - 90	80.2	467	9.1/10	80.1 ± 0.4 ; 2.8 ± 0.5
64 - 92	79.8	468	12.9/11	80.2 ± 0.4 ; 2.8 ± 0.7
64 - 94	79.8	474	18.6/12	80.1 ± 0.3 ; 2.6 ± 0.6
Width Fixed	$\Gamma_W = 2.1$ GeV			
56 - 94	79.5 GeV	609	23.2/17	80.2 ± 0.3 GeV
60 - 94	79.6	548	23.2/15	80.1 ± 0.3
64 - 90	80.0	467	9.6/11	80.1 ± 0.3
64 - 92	79.6	468	14.2/12	80.2 ± 0.3
64 - 94	79.8	474	19.3/13	80.1 ± 0.3

Table 4: Effect of varying the transverse mass fit range on the apparent W mass.

to internal diagrams in the W production [7]. The radiative corrections accurately reproduce the tail of the E/p distribution for electrons, giving confidence in the method. The other systematic errors listed in table 5 are the same as for the electron analysis [1].

$Z^0 \rightarrow \mu^+\mu^-$ Analysis

Selecting dimuon pairs with an invariant mass near M_Z is enough of a constraint that the muon quality cuts can be rather loose. In fact, we extend the angular coverage beyond that of the muon chambers by first selecting high P_t muons, and then looking for a second stiff track with a minimum ionizing signal in the endwall calorimeter beyond the coverage of the chambers ($|\eta| < 1.2$, or, equivalently, 33° from the beam). This increases the acceptance to about 20% of the cross section. As mentioned, another 20% of the Z's have one muon in the muon chambers, and one beyond the range of the central drift chamber using present track reconstruction software. The reconstruction software is being refined to increase the efficiency for tracks traversing only a few of the wire superlayers. Hence, 60% of the Z cross section has neither muon in the muon chambers. (The upgrade plans for the 1991 collider run include extending the angular coverage of the muon chambers.) The Z selection cuts are listed in table 6, see also reference [8]. After all cuts, there are no like-sign muon pairs in the mass range of the

Uncertainty	Electron	Muon
Statistical	200(380)	430(440)
1. Mass Scale	320 MeV	180 MeV
2. Radiative Corrections	100	100
3. Proton Structure	300	300
4. Resolution, p_t W, etc.	400	400
5. Background	≤ 50	≤ 50
6. Binned fitting	250	250
Overall Systematic	650	600
Overall	650(730)	740(750)

Table 5: Systematic errors in the M_W determination.

Cut	Description
Both muons	$p_t > 20$ GeV/c EM < 2.0 GeV, Had < 6.0 GeV in muon tower
First muon	Muon chambers match CTC within 10 cm
Second muon	$\|\eta\| < 1.2$ (beyond muon chambers)
Veto cosmics	Muons not back-to-back, within 1.5° in ϕ and 0.1 in η.
Veto QCD b'grd	No jet, $E_t > 15$ GeV, within $\Delta R < 0.4$

Table 6: Cuts used in selection of $Z^0 \rightarrow \mu^+\mu^-$ events.

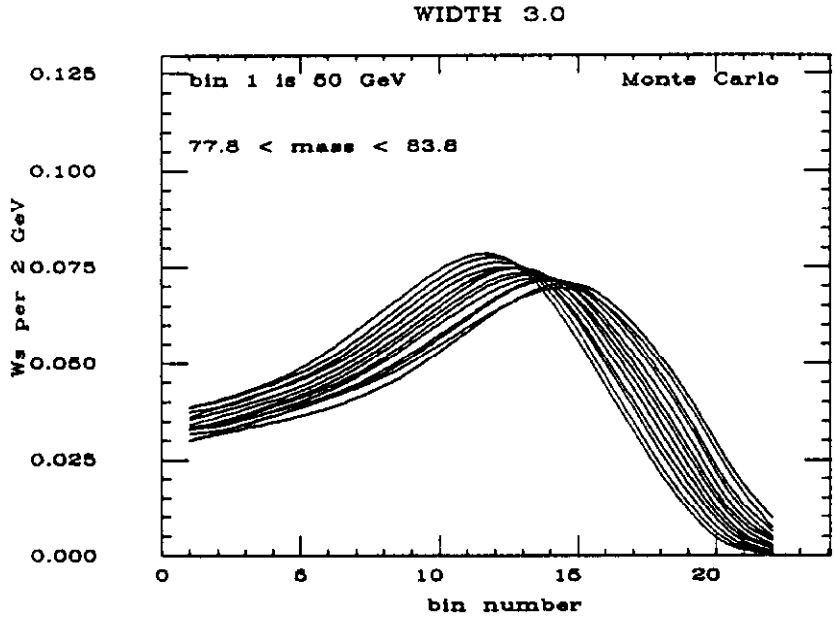

Figure 3: Evolution of the $W \rightarrow \mu\nu$ transverse mass distribution as a function of M_W, for fixed Γ_W.

fit. Figure 5 shows the data after beam-constrained track reconstruction. See reference [1] for a discussion of the tracking systematics. The dimuon invariant mass distribution is fitted with a relativistic Breit-Wigner convoluted with the detector resolution.

The value of the mass obtained from the fit is corrected for the effect of the proton structure functions by adding 80 MeV/c^2. This can be understood as follows: in an e^+e^- experiment the Z mass and width would be measured by counting the number of Z's produced as a function of energy, normalizing to the integrated luminosity at each point of the energy scan, and fitting the points. The luminosity depends, amongst other things, on the number of particles in the beam. Similarly, in a $p\bar{p}$ experiment the beam energy is left fixed, but because the quarks within the proton have momentum distributions, one in fact sees a distribution in dimuon invariant mass, just as in the e^+e^- experiment. However, there are more quarks with a lower fraction of the proton energy (structure functions), and hence the "luminosity" is lower for higher dimuon mass, and a correction has to made. We find the magnitude of the correction by comparing the monte carlo with a flat structure function with physical structure functions. The error in the correction comes from using different structure functions. Using the same radiative

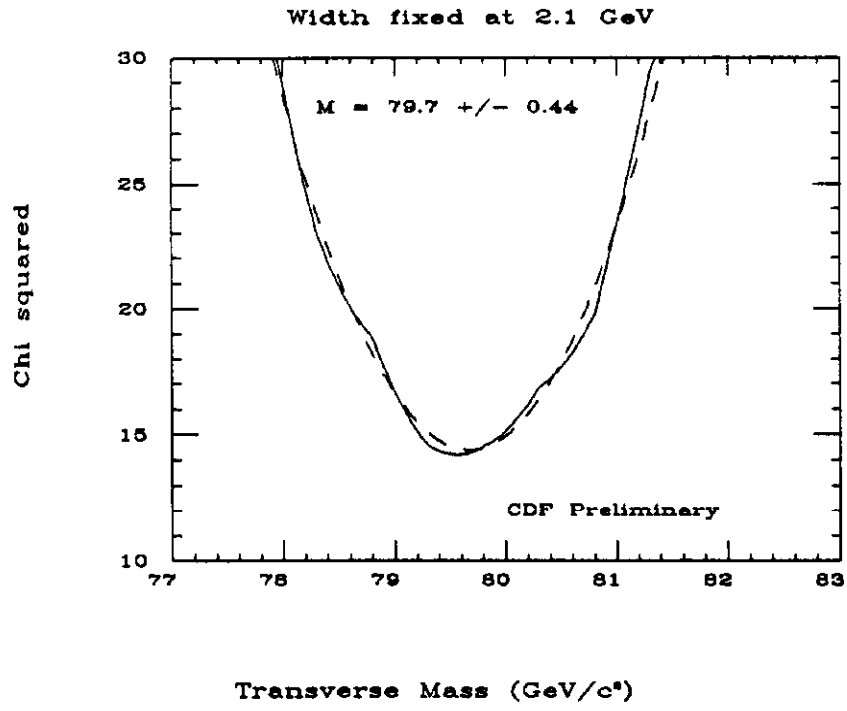

Figure 4: χ^2 as a function of W mass from the fit to the data. Dashed line is a parabolic fit.

correction calculation as for the W's, 220 MeV is added to the fitted M_Z. After all corrections, the measurement of M_Z from the muon channel is $90.7 \pm 0.4 \pm 0.2$ GeV/c^2. The electron measurement yields $91.1 \pm 0.3 \pm 0.4$ GeV/c^2. Combining the two results gives $90.9 \pm 0.3 \pm 0.2$ GeV/c^2, where the first error is statistical and the second error is systematic.

Conclusions

We have described of the mass measurement for the $W^{\pm}$ and Z^0 particles in the muon decay channel, using 4.4 pb^{-1} of proton-antiproton collision data from the Fermilab Tevatron, as measured by CDF. The preliminary value is $M_W = 79.9 \pm 0.4 \pm 0.6$ GeV/c^2, and for the Z^0 we find $M_Z = 90.9 \pm 0.3 \pm 0.2$ GeV/c^2 and $\Gamma_Z = 3.8 \pm 1.1 \pm 1.0$ GeV/c^2.

References

[1] T.J. Phillips *et al.* (CDF Collaboration), "$W^{\pm}$ and Z^0 Masses and Standard Model Parameters at CDF ", these proceedings.

[2] G.S. Abrams *et al.* (Mark-II Collaboration at SLC), Phys. Rev. Lett. **63**, 2173

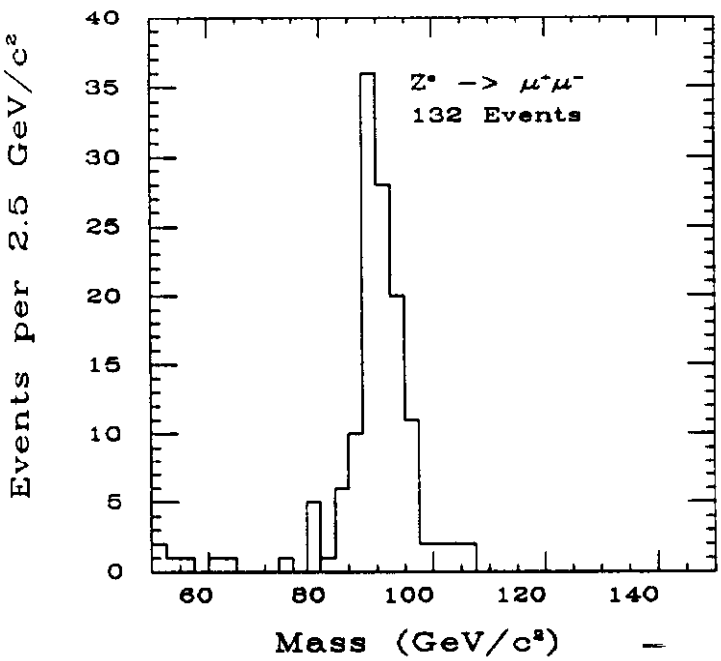

Figure 5: Dimuon invariant mass distribution used to measure M_Z.

(1989); Recent results from ALEPH, DELPHI, L3, and OPAL at LEP (CERN), submitted to Phys. Lett. B.

[3] F. Abe *et al.* (CDF), Nucl. Inst. Meth. **A271**,387 (1988).

[4] CDF internal memo 1025, "A Fast W and Z Monte Carlo", Claudio Campagnari

[5] F. Abe *et al.* (CDF Collaboration), "Measurement of the Ratio $\sigma(W \to e\nu)/\sigma(Z \to ee)$ in $p\bar{p}$ Collisions", submitted to *Phys. Rev. Let.*, December 1989.

[6] F. James and M. Roos, "Function Minimization and Error Analysis", 1983, CERN Program Library Documentation.

[7] R.G.Wagner (unpublished) based on calculations by F. Berends *et al.*, Z. Phys. C. **27**, 155 (1985); F. Berends and R. Kleiss, Z. Phys. C **27**, 365 (1985)

[8]"Measurement of the Mass and Width of the Z^0 Boson at the Fermilab Tevatron", F. Abe et al (The CDF Collaboration) *Phys. Rev. Let.* **63**, 720 (1989)

CDF Collaboration for the 1988-1989 Run

F. Abe,[8] D. Amidei,[4] G. Apollinari,[11] M. Atac,[4] P. Auchincloss,[14] A. R. Baden,[6] A. Bamberger,[19] A. Barbaro-Galtieri,[9] V. E. Barnes,[12] F. Bedeschi,[11] S. Behrends,[2] S. Belforte,[11] G. Bellettini,[11] J. Bellinger,[18] J. Bensinger,[2] A. Beretvas,[4] J. P. Berge,[4] S. Bertolucci,[5] S. Bhadra,[7] M. Binkley,[4] R. Blair,[1] C. Blocker,[2] A. W. Booth,[4] G. Brandenburg,[6] D. Brown,[6] E. Buckley,[14] A. Byon,[12] K. L. Byrum,[18] C. Campagnari,[3] M. Campbell,[3] R. Carey,[6] W. Carithers,[9] D. Carlsmith,[18] J. T. Carroll,[4] R. Cashmore,[19] F. Cervelli,[11] K. Chadwick,[4] G. Chiarelli,[5] W. Chinowsky,[9] S. Cihangir,[4] A. G. Clark,[4] D. Connor,[10] M. Contreras,[2] J. Cooper,[4] M. Cordelli,[5] D. Crane,[4] M. Curatolo,[5] C. Day,[4] S. Dell'Agnello,[11] M. Dell'Orso,[11] L. Demortier,[2] P. F. Derwent,[3] T. Devlin,[14] D. DiBitonto,[15] R. B. Drucker,[9] J. E. Elias,[4] R. Ely,[9] S. Errede,[7] B. Esposito,[5] B. Flaugher,[14] G. W. Foster,[4] M. Franklin,[6] J. Freeman,[4] H. Frisch,[3] Y. Fukui,[8] Y. Funayama,[16] A. F. Garfinkel,[12] A. Gauthier,[7] S. Geer,[6] P. Giannetti,[11] N. Giokaris,[13] P. Giromini,[5] L. Gladney,[10] M. Gold,[9] K. Goulianos,[13] H. Grassmann,[11] C. Grosso-Pilcher,[3] C. Haber,[9] S. R. Hahn,[4] R. Handler,[18] K. Hara,[16] R. M. Harris,[9] J. Hauser,[3] T. Hessing,[15] R. Hollebeek,[10] L. Holloway,[7] P. Hu,[14] B. Hubbard,[9] B. T. Huffman,[12] R. Hughes,[10] P. Hurst,[7] J. Huth,[4] M. Incagli,[11] T. Ino,[16] H. Iso,[16] H. Jensen,[4] C. P. Jessop,[6] R. P. Johnson,[4] U. Joshi,[4] R. W. Kadel,[4] T. Kamon,[15] S. Kanda,[16] D. A. Kardelis,[7] I. Karliner,[7] E. Kearns,[6] R. Kephart,[4] P. Kesten,[2] R. M. Keup,[7] H. Keutelian,[7] S. Kim,[16] L. Kirsch,[2] K. Kondo,[16] S. E. Kuhlmann,[1] E. Kuns,[14] A. T. Laasanen,[12] J. I. Lamoureux,[18] W. Li,[1] T. M. Liss,[7] N. Lockyer,[10] C. B. Luchini,[7] P. Maas,[4] M. Mangano[11] J. P. Marriner,[4] R. Markeloff,[18] L. A. Markosky,[18] R. Mattingly,[2] P. McIntyre,[15] A. Menzione,[11] T. Meyer,[15] S. Mikamo,[8] M. Miller,[3] T. Mimashi,[16] S. Miscetti,[5] M. Mishina,[8] S. Miyashita,[16] Y. Morita,[16] S. Moulding,[2] A. Mukherjee,[4] L. F. Nakae,[2] I. Nakano,[16] C. Nelson,[4] C. Newman-Holmes,[4] J. S. T. Ng,[6] M. Ninomiya,[16] L. Nodulman,[1] S. Ogawa,[16] R. Paoletti,[11] A. Para,[4] E. Pare,[6] J. Patrick,[4] T. J. Phillips,[6] R. Plunkett,[4] L. Pondrom,[18] J. Proudfoot,[1] G. Punzi,[11] D. Quarrie,[4] K. Ragan,[10] G. Redlinger,[3] J. Rhoades,[18] M. Roach,[17] F. Rimondi,[19] L. Ristori,[11] T. Rohaly,[10] A. Roodman,[3] A. Sansoni,[5] R. D. Sard,[7] A. Savoy-Navarro,[19] V. Scarpine,[7] P. Schlabach,[7] E. E. Schmidt,[4] M. H. Schub,[12] R. Schwitters,[6] A. Scribano,[11] S. Segler,[4] Y. Seiya,[16] M. Sekiguchi,[16] P. Sestini,[11] M. Shapiro,[6] M. Sheaff,[18] M. Shochet,[3] J. Siegrist,[9] P. Sinervo,[10] J. Skarha,[18] K. Sliwa,[17] D. A. Smith,[11] F. D. Snider,[3] R. St. Denis,[6] A. Stefanini,[11] R. L. Swartz, Jr.,[7] M. Takano,[16] K. Takikawa,[16] S. Tarem,[2] D. Theriot,[4] M. Timko,[15] P. Tipton,[9] S. Tkaczyk,[4] A. Tollestrup,[4] G. Tonelli,[11] J. Tonnison,[12] W. Trischuk,[6] Y. Tsay,[3] F. Ukegawa,[16] D. Underwood,[1] R. Vidal,[4] R. G. Wagner,[1] R. L. Wagner,[4] J. Walsh,[10] T. Watts,[14] R. Webb,[15] C. Wendt,[18] W. C. Wester, III,[9] T. Westhusing,[11] S. N. White,[13] A. B. Wicklund,[1] H. H. Williams,[10] B. L. Winer,[9] A. Yagil,[4] A. Yamashita,[16] K. Yasuoka,[16] G. P. Yeh,[4] J. Yoh,[4] M. Yokoyama,[16] J. C. Yun,[4] F. Zetti[11]

[1] Argonne National Laboratory, Argonne, Illinois 60439
[2] Brandeis University, Waltham, Massachusetts 02254
[3] University of Chicago, Chicago, Illinois 60637
[4] Fermi National Accelerator Laboratory, Batavia, Illinois 60510
[5] Laboratori Nazionali di Frascati, Istituto Nazionale di Fisica Nucleare, Frascati, Italy
[6] Harvard University, Cambridge, Massachusetts 02138
[7] University of Illinois, Urbana, Illinois 61801
[8] National Laboratory for High Energy Physics (KEK), Tsukuba, Ibaraki 305, Japan
[9] Lawrence Berkeley Laboratory, Berkeley, California 94720
[10] University of Pennsylvania, Philadelphia, Pennsylvania 19104
[11] Istituto Nazionale di Fisica Nucleare, University and Scuola Normale Superiore of Pisa, I-56100 Pisa, Italy
[12] Purdue University, West Lafayette, Indiana 47907
[13] Rockefeller University, New York, New York 10021
[14] Rutgers University, Piscataway, New Jersey 08854
[15] Texas A&M University, College Station, Texas 77843
[16] University of Tsukuba, Tsukuba, Ibaraki 305, Japan
[17] Tufts University, Medford, Massachusetts 02155
[18] University of Wisconsin, Madison, Wisconsin 53706
[19] Visitor